Advanced Materials Research Vol. 922 (2014) pp 189-194
Online available since 2014/May/07 at www.scientific.net

doi:10.4028/www.scientific.net/AMR.922.189

Effect of plastic deformation on a dispersion of omega-phase and mechanical properties of an Al-Cu-Mg-Ag alloy

Marat Gazizov[a], Ivan Zuiko[b], Rustam Kaibyshev[c]

Laboratory of Mechanical Properties of Nanostructured Materials and Superalloys, Belgorod State University, Pobeda 85, Belgorod, 308015, Russia

[a]gazizov@bsu.edu.ru, [b]zuiko_ivan@bsu.edu.ru, [c]rustam_kaibyshev@bsu.edu.ru

Keywords: Aluminum alloys; Cold working; Precipitation; Microstructure; Mechanical properties.

Abstract. Effect of cold rolling prior to ageing on a dispersion of secondary phases and mechanical properties at room temperature for an Al-5.6Cu-0.72Mg-0.5Ag-0.32Mn-0.17Sc-0.12Zr (wt. %) alloy, which was solution treated and water quenched initially, was examined. It was shown that cold working leads to significant increase in density of lattice dislocations that induces the formation discrete agglomerates of the θ′-phase on the {100} planes. Strain of 7% provided increased aspect ratio (length to thickness) of plates that leads to moderate increase of strength. Imposing of higher strains leads to increased lattice dislocation density and the formation of deformation-induced boundaries. Precipitation of the coarse particles of secondary phases on these boundaries takes place. The high yield stress (YS) of 535 MPa and ultimate tensile strength (UTS) of 570 MPa, were attained after cold rolling with a reduction of 80% followed by ageing at 190°C for 2 h. The effect of plastic deformation prior to ageing on the precipitation behavior and strengthening of Al-Cu-Mg-Ag alloy is discussed.

Introduction

The aluminum alloys belonging to Al-Cu-Mg-Ag system exhibit excellent mechanical properties at room and elevated temperatures that make it possible to consider them as a material for use in aerospace industries for structures operating at elevated temperatures [1-3].Artificial aging of Al-Cu-Mg-Ag alloys results in the precipitation of several transition phases as Al_2Cu (θ′), Al_2Cu(Ω) with monoatomic flat interface segregations of Mg-Ag and thermodynamically equilibrium phases as Al_2Cu (θ), which are distinctly distinguished by morphology and their contribution to overall dispersion hardening [2,4]. In peak aged Al-Cu-Mg-Ag alloys the precipitation of a finely dispersed predominant Ω-phase and minor θ′-phase occurs. The Ω- and θ′-phase forms as plates on the $\{111\}_\alpha$ and $\{001\}_\alpha$ planes, respectively [4,5]. Theoretical calculations having excellent agreement with experimental observations conclude that the appearance condition of the maximum increment to critical resolved shear stress (CRSS) for alloys containing disperse particles is superposition of such important mechanisms contributing to strength as interfacial strengthening, order strengthening and Orowan strengthening. This condition is depended on precipitate parameters (volume fraction, distribution, interfacial energy, plate length, plate thickness, etc.) [6,7].For given volume fraction and number density of shear-resistant plate-shaped precipitates per unit volume, the increment in CRSS produced by $\{111\}_\alpha$ plates is invariably larger than that produced by $\{001\}_\alpha$ plates and, for both precipitate orientations strengthening increment increases with an increase in plate aspect ratio [6].

The relative precipitation kinetics of θ′, θ and Ω particles may be affected by the introduction of plastic deformation prior to ageing [5]. The plastic deformation of age-hardenable aluminum alloys prior to ageing generally leads to increased density of crystallographic defects and accelerate the diffusion of solute atoms [8,9]. Whereas, the deformation-induced boundaries are predominant places for precipitation of coarse secondary phase after prolonged soaking at high temperature [8,9]. These phases are usually thermodynamically equilibrium phases and give no contribution to overall dispersion hardening [8].

The aim of this paper is to report the effect of cold rolling and subsequent artificial ageing on the precipitation behavior and strengthening of an Al-Cu-Mg-Ag alloy.

Experimental details

An aluminum alloy with a chemical composition of Al-5.6Cu-0.72Mg-0.5Ag-0.32Mn-0.17Sc-0.12Zr-0.1Ge (wt %) was prepared by semi-continuous casting. Initially, ingots with dimensions of ∅40 mm×120 mm were subjected to a two-step homogenization annealing at 360°C for 6 h, followed by subsequent heating to 510°C and soaking for 24 h [10]. After two-step homogenization annealing the ingots were forged at 400°C with a strain of 75% to produce rectangular billets. Rods with dimensions of 20 mm×20 mm×100 mm were machined from these billets parallel to the major axis. These rods were solution treated at 525°C for 1 h followed by water quenching.

The specimens for tensile were prepared from parts of solution treated rods and them stretched by plastic strain (PS) of 1, 3, 5 and 7%. Other parts of solution treated rods were cold rolled with reductions of 20, 40 and 80%. For attaining the peak ageing condition the cold deformed samples were immediately aged at 190°C from 0.5 to 96 h.

The hardness measurements were carried out at room temperature by using Vickers hardness tester with a load 2 N. The tensile tests were conducted at room temperature at a constant rate of crosshead displacement, with initial strain rate equal to 1.3×10^{-3} s^{-1}. The flat "dogbone" specimens with 25 mm gauge length, 7 mm width and 3 mm thickness were used. The major tensile axes were parallel to the rolling or tension directions. The flat surfaces of specimens were ground wet with SiC abrasive paper having finish grit size 2400# (FEPA) before tests.

Specimens for microstructural characterization were prepared from gauge length sections parallel to the major axis of the samples. The microstructures were examined using a JEOL JEM-2100 transmission electron microscope with accelerating potential of 200 kV in bright field(BF-TEM) mode. The TEM specimens were mechanically ground wet to a thickness of about ~150 μm and finally electropolished at 20 V in a solution of 30%-HNO_3 and 70%-CH_3OH at a temperature of -30°C using a Tenupol-5 twin-jet polishing unit.

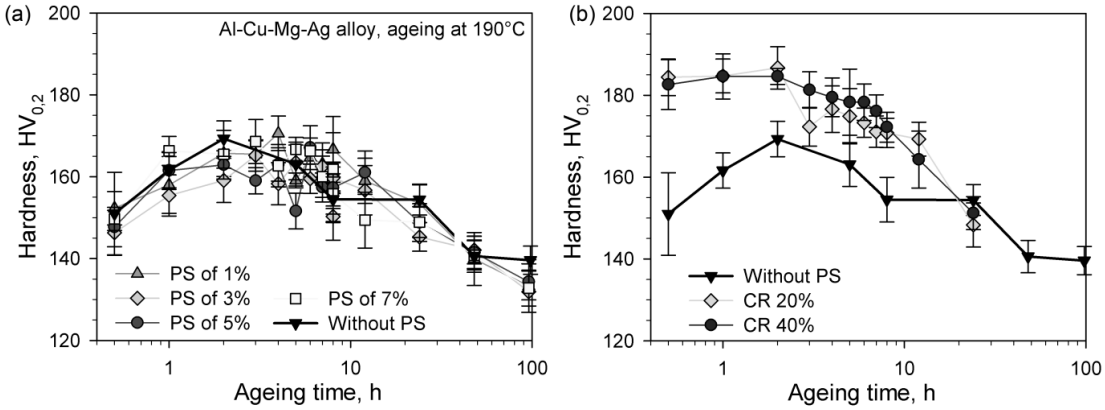

Fig. 1 Effect of cold deformation as tensile (a) and cold rolling (b) on the ageing response measured by a Vickers hardness tester at room temperature.

Quantitative microstructural characterization and statistical interpretation of particles were carried out. The apparent diameter (D) and thickness (h) of each particle were measured from BF-TEM images with the electron beam orientated parallel to the$<011>_\alpha$zone axis of the matrix. About 200-300 measurements for each condition were carried out for the statistical purpose. Average number density of particles (N) was calculated taking into account the number of particles of Ω phase precipitated on two $\{111\}_\alpha$ planes and finally multiplied by 1.5 and divided by the area of the view area and foil thickness, which was measured by the convergent electron beam diffraction (CBED) method described in work [11].The errors associated with measurements of the diameter and thickness of Ω plates are listed based on the particle size distributions. The real error of measurements is much less.

Results and discussion

Hardness. Fig. 1 shows the ageing response at 190°C for the alloy after different types of prior cold deformation. In general, there is no effect of tension on the peak age-hardening level which is

~165 HV (Fig. 1a). In contrast, cold rolling affects microhardness. The hardness increase up to ~185 HV was observed for samples subjected to cold rolling with reductions of 20 or 40% followed by short aging (Fig. 1b). The prolonged ageing at the same temperature leads to the elimination of this positive effect; after 20 h the hardness of all samples is the same (Fig.1b). It should be noted that the acceleration of precipitation kinetics take place for the rolled samples, but peak-ageing condition (190°C, 2 h) is the same for the all treatments. Keeping of hardness on high level after prolonged soaking at relatively high temperature indicates that experimental alloy has excellent heat-resistant properties.

Table 1 Effect of cold deformation on the tensile properties

Treatment	YS, σ_{YS} [MPa]	UTS, σ_{UTS} [MPa]	Uniform elongation, δ_{UE} [%]	Elongation to failure, δ [%]	σ_{YS}/σ_{UTS}	CRSS, σ_{YS}/M [MPa]
Solution treatment	145	370	20	22	0.392	47
Ageing at 190°C for 2 h (T6)	450	495	5.5	8.9	0.909	147
Tension to PS of 1% and ageing at 190°C for 2 h.	440	485	5.4	8.6	0.907	144
Tension to PS of 3% and ageing at 190°C for 2 h.	460	495	5.5	8.4	0.929	150
Tension to PS of 5% and ageing at 190°C for 2 h.	465	495	5.8	7.7	0.939	150
Tension to PS of 7% and ageing at 190°C for 2 h.	480	515	6.4	9.4	0.932	157
Tension to PS of 10% and ageing at 190°C for 2 h.	480	510	4.2	6.8	0.941	157
Cold rolling with reduction of 20% and ageing at 190°C for 2 h.	505	530	3.7	6.5	0.953	165
Cold rolling with reduction of 40% and ageing at 190°C for 2 h.	530	560	4.7	7.1	0.946	173
Cold rolling with reduction of 80% and ageing at 190°C for 2 h.	535	570	3.9	5.9	0.939	175

Tensile properties. The results of tension tests are summarized in Table 1. Baseline determination of mechanical properties after ageing at 190°C for 2 h (T6 temper) shows that the yield stress (YS) of 450 MPa, ultimate tensile strength (UTS) of 495 MPa with elongation to failure of ~9% can be achieved in present alloy without prior plastic deformation. It is seen that there is a negative effect of plastic strain of 1% by tension on strength after ageing. Further increase of plastic strain from 3% to 80% leads to gradual strength increase. The experimental alloy after cold rolling with a reduction of 80% and ageing at 190°C for 2 h demonstrates highest values of YS of ~535 MPa, UTS of ~560 MPa and elongation to failure of ~7%. Experimental values of the increments in CRSS attributed to the all strengthening mechanisms can be determined as σ_{YS}/M, where σ_{YS} is the YS, M= 3.06 is the Taylor factor for polycrystalline fcc alloys with random texture [6].

Microstructure. The full details of the nature, average size, shape and distribution of the secondary phases in the homogenized and solution treated alloy were previously described in detail [10].

The microstructure of the solution treated alloy consisted of initial grains having average dimensions of ~48 and ~30 μm in the longitudinal and transverse directions, respectively. Coarse particles of the primary θ-phase and ternary W-phase ($Al_{8-x}Cu_{4+x}Sc$) were situated on grain

boundaries [10]. It is worth noting that the coherent particles of the $Al_3(Sc,Zr)$ phase having average size of ~25 nm were non-uniformly distributed within interiors of grains [10].

Table 2 Effect of tempers on the precipitate parameters of the Ω-phase within grain interiors

Condition	Length, D [nm]	Thickness, h [nm]	Aspect ratio, A	$\Delta\tau_{IS}$ [MPa]	$\Delta\tau_{OrdS}$ [MPa]
Ageing at 190°C for 2 h (T6)	23.9±11.7	1.6±0.4	14.15±3.17	15	84
Tension to PS of 7% and ageing at 190°C for 2 h.	30.8±14.5	1.0±0.3	29.67±2.49	50	77
Cold rolling with reduction of 80% and ageing at 190°C for 2 h.	25.3±9.8	1.0±0.3	25.11±1.51	41	75

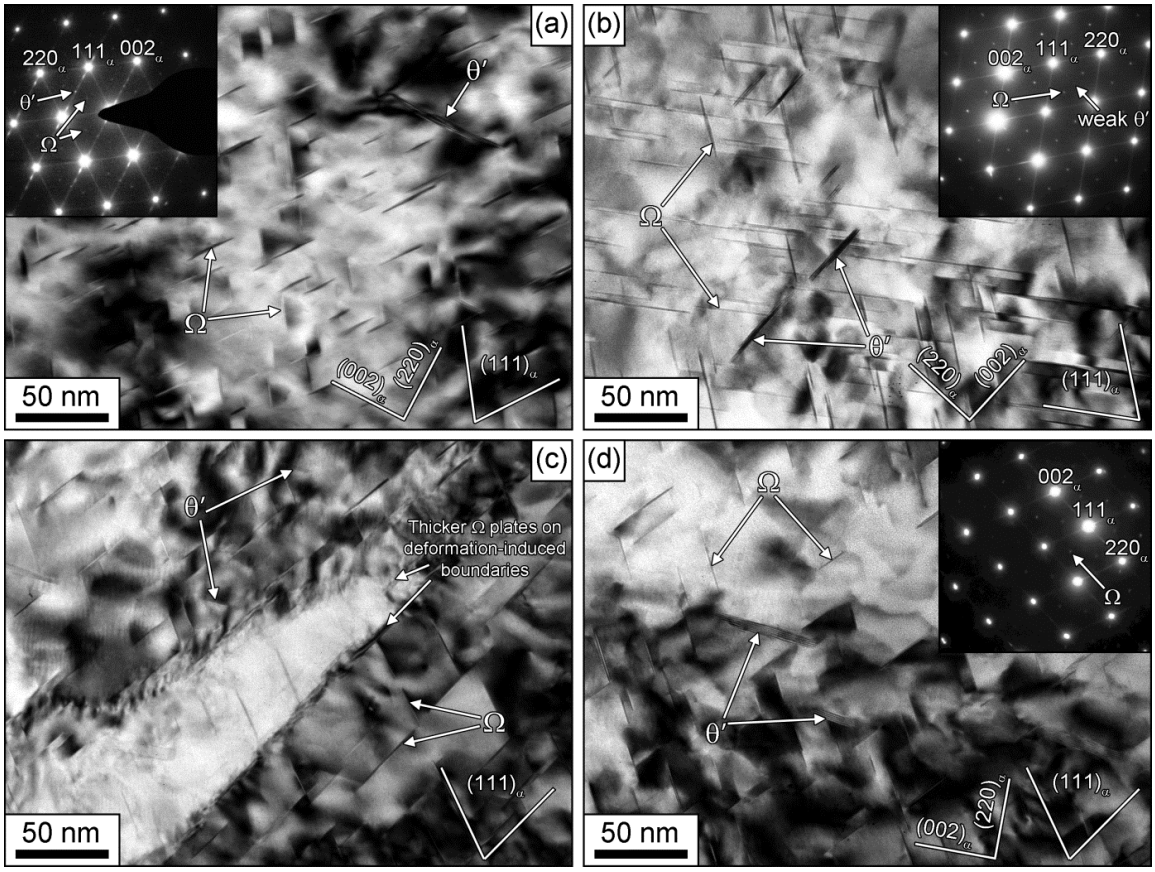

Fig. 2 <110>$_\alpha$ BF-TEM images of samples after no prior strain followed by ageing at 190°C for 2 h (a), a prior strain of 7% followed by ageing at 190°C for 2 h (b), a prior strain of 80% followed by ageing at 190°C for 2 h (d)

Fig. 2 shows a series of <110>$_\alpha$ BF-TEM images and SAED patterns of precipitation structures after cold deformation and ageing at 190°C for 2 h. The particles aligned along the $\{110\}_\alpha$ planes were identified as Ω-phase. Values of the length (*D*), thickness (*h*) and number density (*N*) of the Ω particles within grain interiors are listed in Table 2. There is the conspicuous effect of cold deformation on the morphology of the Ω-phase particles. The aspect ratio (length to thickness) is dependent on strain and increases from 14.2±3.2 for T6 sample to 29.7±2.5 for treatment with PS of 7% and ageing at 190°C for 2 h (Table 2, Figs. 2a and b). This effect results from thinning of the Ω plates due to prior strain (Figs. 2c and d). The precipitation of thicker Ω-plates on the deformation-induced boundaries takes place. It is worth noting that homogeneous nucleation of the Ω-phase takes place with and without strain.

It should be noted that the other particles aligned along the $\{001\}_\alpha$ planes were identified as θ′-phase. After ageing the density of these particles is negligible for unstrained samples. Tensile

strains lead to heterogeneous precipitation of the thin plates of θ′-phase as discrete conglomerates on the lattice dislocations (Fig. 2b).

The increments in CRSS were calculated for mechanisms of interfacial strengthening, order strengthening, and Orowan strengthening. The contribution of the matrix phase (τ_m) to the CRSS of the alloy was typically assumed to be of the order of 10 MPa [12]. The increment in CRSS due to Orowan strengthening mechanism is given by [6]:

$$\Delta\tau_{OS} = \left\{\frac{Gb}{2\pi\sqrt{1-\nu}}\right\}\left\{\frac{1}{0.931\Delta\tau IS\sqrt{\frac{0.265\pi Dh}{f}-\frac{\pi D}{8}-0.919h}}\right\}\left\{\ln\frac{1.061h}{r_o}\right\}. \quad (1)$$

where G is the shear modulus of the Al matrix phase, b is the Burgers vector of the slip dislocations, ν is Poisson's ratio, D and h is average length and thickness of plate-like particles, r_o is the core radius of dislocations, f = 0.054 is the volume fraction of particles. In present analysis, G = 25 GPa, b= 0.286 nm, ν = ⅓ [6], r_o = ¾b = 0.215 nm. The substitution of these values and precipitate parameters from Table 2 into Eq. 1 leads to increments in CRSS of 245, 305 and 295 MPa for T6 condition, and samples subjected to prior strains of and 80%, respectively, followed by the aging. The contribution of this mechanism is significantly higher than values of total CRSS for aged samples (Table 1) and cannot be considered as operative.

The increment in CRSS due to interfacial strengthening for an alloy containing shearable $\{111\}_\alpha$ plates can be written in form:

$$\Delta\tau_{IS} = \frac{1.211D}{h^2}\left(\frac{bf}{\Gamma}\right)\gamma_i^{3/2} \quad (2)$$

where γ_i is the specific interfacial energy between precipitate and matrix phases (currently accepted values for specific precipitate/matrix energy vary in range 0.01 to 0.1 J/m^2[6]), Γ is the dislocation line tension given by [6]:

$$\Gamma = \frac{Gb^2}{2\pi}\ln\sqrt{\frac{D^2}{2b^2f}} \quad (3)$$

In present analysis, $\gamma_i \sim 0.06$ J/m^2 was used for calculations.

The contribution of order strengthening to CRSS is given by an equation of the form [7]:

$$\Delta\tau_{OrdS} = \left(\frac{\gamma_{apb}}{2b}\right)\left\{\left(\frac{2fh\gamma_{apb}}{\pi\Gamma}\left(\frac{A\sqrt{6}}{3}\right)^{1/2}\right)^{1/2} - Cf\right\} \quad (4)$$

where A is an aspect ratio of the $\{111\}_\alpha$ plates, γ_{apb} is specific antiphase boundary energy on the slip plane of the precipitate phase, C = 1/3 is a constant for alloy aged with no stress [14]. The value of γ_{apb} = 0.3 J/m^2 was used for theoretical calculations. Substituting Eq. 3 into Eq. 2 and 4 allows calculating variation of the increments in CRSS for the different precipitates. These values calculated are summarized in Table 2.

Thereby, the Al-Cu-Mg-Ag alloy had been subjected cold working up to a strain of80% followed by artificial ageing at 190°C. It was found that cold working effects on the precipitation behavior and strength of the peak aged alloy. Careful examination of the microstructures has revealed that the minor plastic strains leads to increased aspect ratio by the significant thinning of Ω plates. Present calculation does not consider the formation of atom segregates on crystallographic defects at the expense of the supersaturated solid solution required for the precipitation of the Ω-plates in cold worked samples. However, in the first approximation it allows comparing the strengthening effect of the Ω plates with different dimensions. The derived values show that thinning of the Ω plates leads to strength increment in CRSS due to modification of morphology of precipitates. At high strains, the precipitation hardening does not increase strengthening significantly, which is confirmed by the experimental results. Increase of dislocation density and formation of the deformation-induced boundaries are main reasons for strengthening of such alloy after prior plastic deformation to high strain and following artificial ageing. It is apparent that the

chains of thicker nanoscale particles of the Ω-phases on deformation-induced boundaries makes them non-transparent for gliding dislocations and these boundaries contribute to grain size strengthening in accordance with Hall-Petch equation.

Summary

It was shown that an increase in strength of Al–Cu–Mg–Ag alloy could be achieved changes in a dispersion of secondary phases through plastic deformation prior to ageing. The effect of strain on aspect ratio of the Ω-phase plates is observed. The alloy subjected to cold rolling with a reduction of 80% followed by ageing at 190°C for 2 h demonstrates YS of ~535 MPa, UTS of ~ 570 MPa and elongation to failure of ~6%.

Acknowledgements

This study was supported by the Ministry for Education and Science of Russia, project 14.A18.21.0442.The authors are grateful to the staff of the Joint Research Center, Belgorod State University, for their assistance with the mechanical and structural characterizations.

References

[1] I.J. Polmear, G. Pons, Y. Barbaux, H. Octor, C. Sanchez, A..J. Morton, W.E. Borbidge, S. Rogers, After Concorde: Evaluation of creep resistant Al-Cu-Mg-Ag alloys, Mater. Sci. Tech. 15 (1999) 861-868.

[2] D. Bakavos, P.B. Prangnell, B. Bes, F. Eberl, The effect of silver on microstructural evolution in two 2xxx series Al-alloys with a high Cu:Mg ratio during ageing to a T8 temper, Mater. Sci. Eng. A491 (2008) 214-223.

[3] M. Vural, J. Caro, Experimental analysis and constitutive modeling for the newly developed 2139-T8 alloy, Mater. Sci. Eng. A520 (2009) 56-65.

[4] S.C. Wang, M.J. Starink, Precipitates and intermetallic phases in precipitation hardening Al–Cu–Mg–(Li) based alloys, Int. Mater. Rev. 50 (2005) 193-215.

[5] S.P. Ringer, B.C. Muddle, I.J. Polmear, Effects of cold work on precipitation in Al-Cu-Mg-(Ag) and Al-Cu-Li-(Mg-Ag) alloys, Metall. Mater. Trans. 26A (1995) 1659-1671

[6] F.J. Nie, B.C. Muddle, Microstructural design of high-strength aluminum alloys, J. Ph. Equilib. 19 (1998) 543-551.

[7] F.J. Nie, B.C. Muddle, Comments on the ”Dislocation interaction with semicoherent precipitates (Ω phase) in deformed Al-Cu-Mg-Ag alloy”, Scr. Mater. 42 (2000) 409-413.

[8] D.A. Porter, K.E. Esterling, M. Sherif, Phase Transformation in Metals and Alloys, third ed., CRS Press, 2009.

[9] R.N. Lumley, A.J. Morton, I.J. Polmear, Enhanced creep performance in an Al-Cu-Mg-Ag alloy through underageing, Acta Mater. 50 (2002) 3597-3608.

[10] M. Gazizov, V. Teleshov, V. Zakharov, R. Kaibyshev, Solidification behaviour and the effects of homogenisation on the structure of an Al-Cu-Mg-Ag-Sc alloy, J. Alloys Compd. 509 (2011) 9497-9507

[11] B.D. Williams, C.B. Carter, Transmission Electron Microscopy, third ed., Springer, New York, 2009

[12] L.E Mondolfo, Aluminium Alloys: Structure and Properties, Butterworths, London, 1976.

[13] W.P. Mason, Drag on dislocations due to thermal losses of the phonon-phonon interaction type, J. Appl. Phys. 35(9) (1964) 2779-2781.

[14] J.M. Oblak, D.F. Paulonis, D.S. Duvall, Coherency strengthening in Ni base alloys hardened by DO22 γ′ precipitates, Metall. Trans. 5(1) (1974) 143-153.

THERMEC 2013 Supplement
10.4028/www.scientific.net/AMR.922

Effect of Plastic Deformation on a Dispersion of Omega-Phase and Mechanical Properties of an Al-Cu-Mg-Ag Alloy

10.4028/www.scientific.net/AMR.922.189